Stem Cell Reports, Volume *5*

Supplemental Information

Activity and High-Order Effective Connectivity Alterations in Sanfilippo C Patient-Specific Neuronal Networks

Isaac Canals, Jordi Soriano, Javier G. Orlandi, Roger Torrent, Yvonne Richaud-Patin, Senda Jiménez-Delgado, Simone Merlin, Antonia Follenzi, Antonella Consiglio, Lluïsa Vilageliu, Daniel Grinberg, and Angel Raya

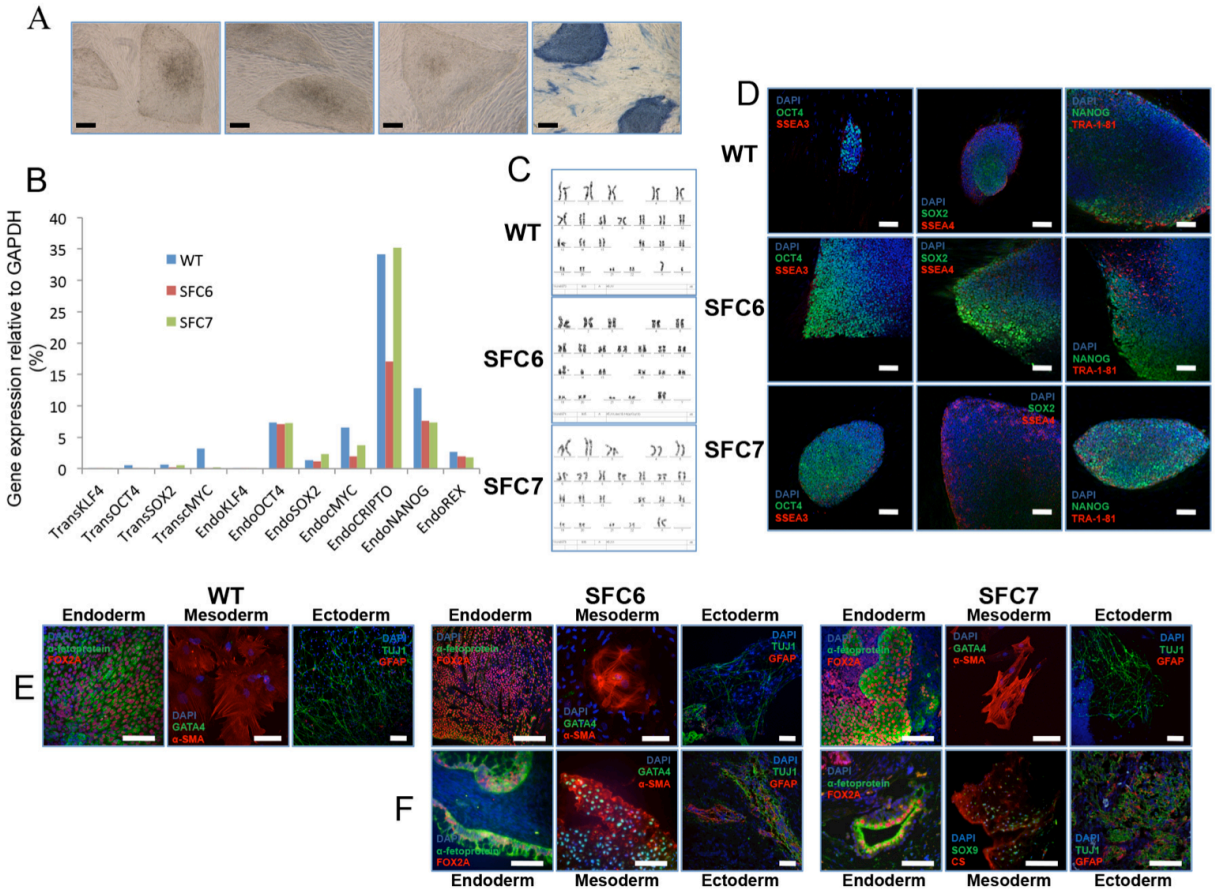

Figure S1. Generation and characterization of control and SFC-iPSC lines using 4 reprogramming factors, Related to Figure 1. A total of 32 independent iPSC lines were obtained after reprogramming control (WT1 and WT2) and SFC (SFC6 and SFC7) fibroblasts with retroviruses expressing *OCT4*, *SOX2*, *KLF4*, and c-*MYC*. Two lines per fibroblast sample were selected for complete characterization: WT1-iPS#4.10, WT1-iPS#4.12, WT2-iPS#4.2, WT2-iPS#4.5, SFC6-iPS#4.6, SFC6-iPS#4.7, SFC7-iPS#4.8, and SFC7-iPS#4.9. Shown are representative images of the characterization of WT (WT1-iPS#4.10), SFC6 (SFC6-iPS#4.6), and SFC7 (SFC7-iPS#4.9) iPSC lines. (A) Typical hESC-like colonies obtained after reprogramming of SFC fibroblasts and positive AP staining of the hESC-like SFC-iPSC colonies (right image). Scale bar: 400 μm. (B) RT-qPCR analyses of the expression levels the indicated retroviral-derived reprogramming factors (TRANS-) and endogenous (ENDO-) genes in WT-, SFC6- and SFC7-iPSC. (C) Karyotype of WT-, SFC6- and SFC7-iPSC, which are identical to that of parent fibroblasts [including the known balanced Robertsonian translocation der(13;14)(q10;q10) of SFC6]. (D) Representative colonies of WT-, SFC6- and SFC7-iPSC stained positive for the pluripotency markers OCT4, SOX2 and NANOG (green), SSEA3, SSEA4 and TRA-1-81 (red). Scale bar: 100 μm. (E) Immunofluorescence analyses with specific markers, on f WT-, SFC6- and SFC7-iPSC differentiated *in vitro* to generate cell derivatives of all three primary germ layers. Endoderm: α-fetoprotein (green), FOX2A (red); mesoderm: GATA4 (green), α-SMA (red); and ectoderm: TUJ1 fetoprotein (green), GFAP (red). Scale bar: 100 μm. (F) Immunofluorescence analyses with specific markers, on sections from a teratoma induced after injecting WT-, SFC6- or SFC7-iPSC, showing cell derivatives of the three embryo germ. Endoderm:α-fetoprotein (green), FOX2A (red); mesoderm: SOX9 (green), CS (red); and ectoderm: TUJ1 fetoprotein (green), GFAP (red). Scale bar: 100 μm.

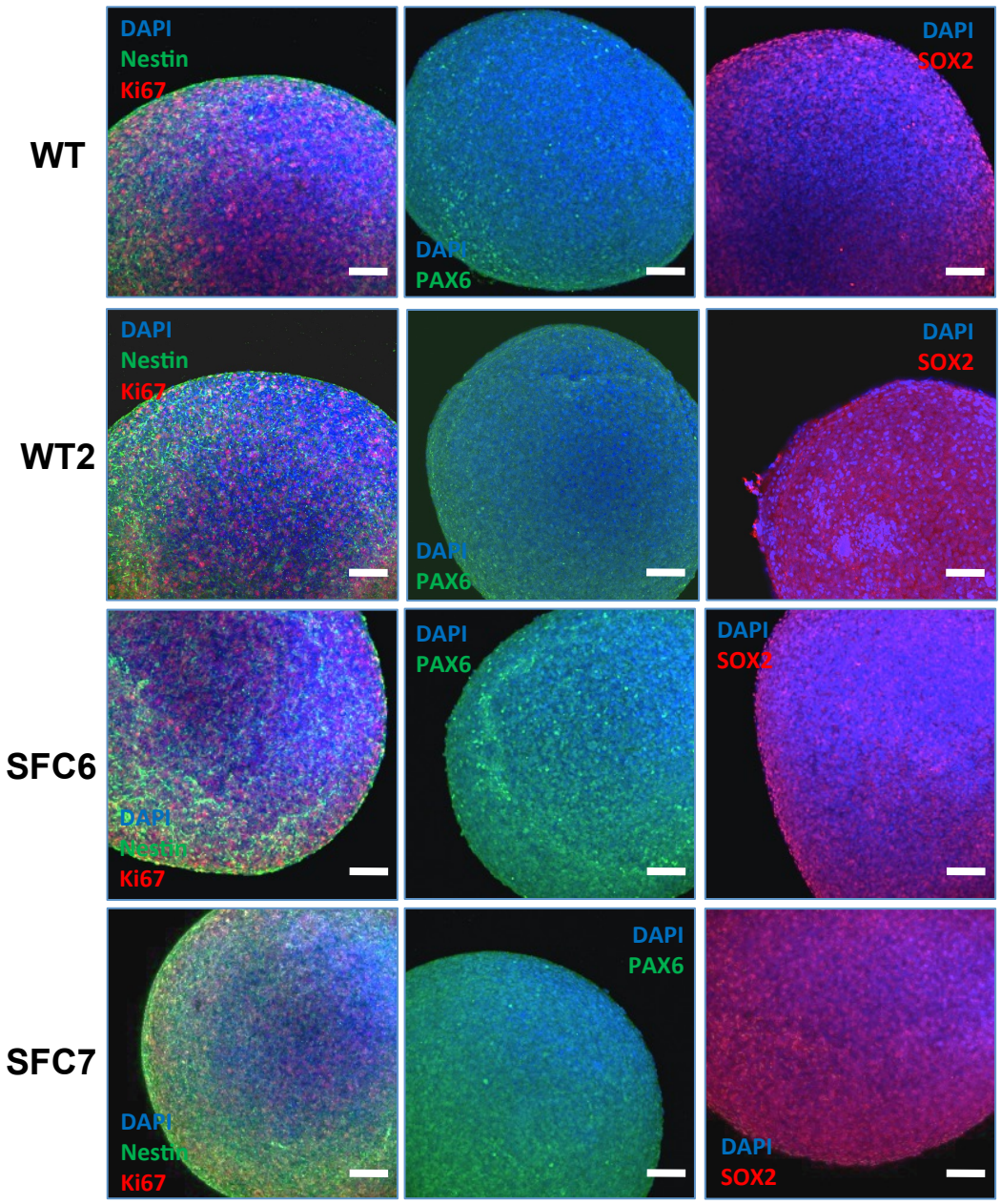

Figure S2. Expression of lineage-specific and proliferation markers in iPSC-derived spherical neural masses (SNMs), Related to Figure 2. SNMs were established from 4 iPSC lines representing each control (WT1 and WT2) and SFC (SFC6 and SFC7) individual. Shown are representative immunoanalysis images of SNMs derived from WT1-iPS#3.6 (WT), WT2-iPS#3.1 (WT2), SFC6-iPS#3.1 (SFC6), and SFC7-iPS#3.1 (SFC7) iPSC lines. Antibodies against Nestin (green) and Ki67 (red) were used in the left images; against PAX6 (green) in the central images, and against SOX2 (red) in the right images. DAPI was used to stain the nuclei (blue). Scale bar: 100 µm.

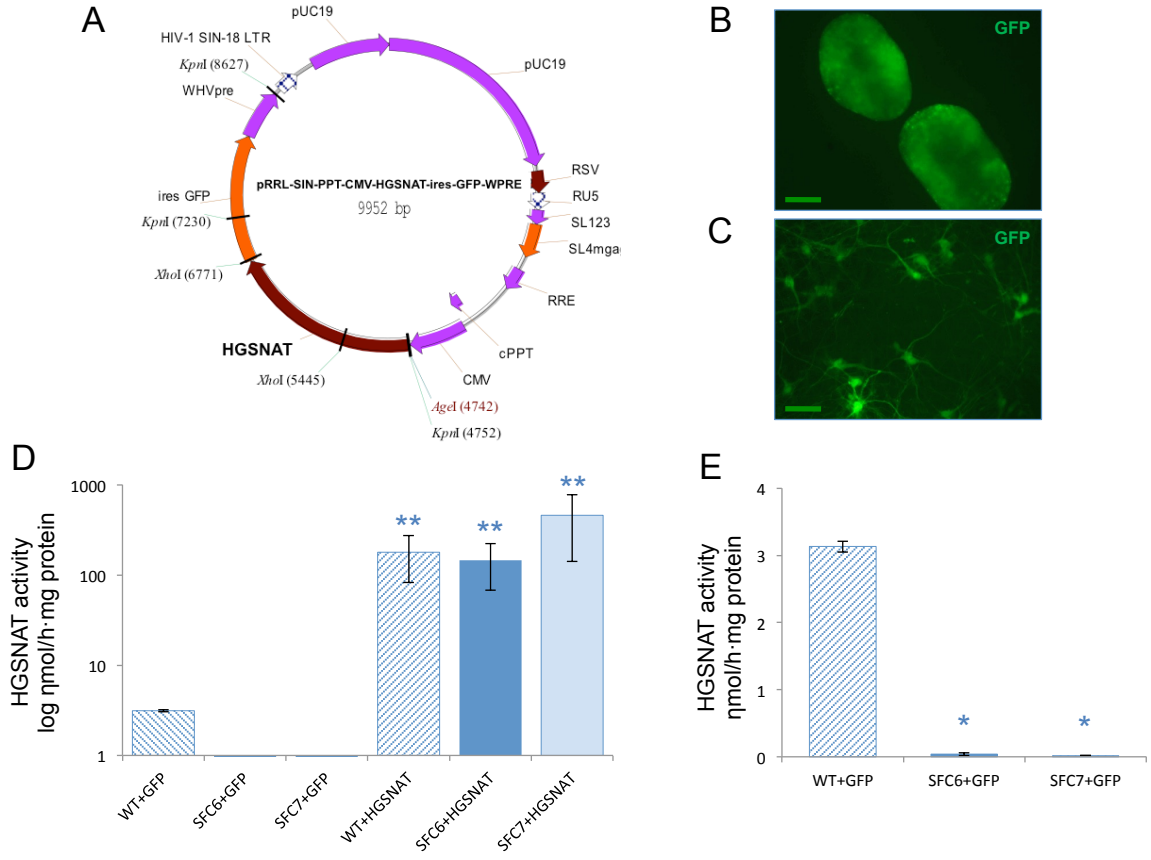

Figure S3. Generation of gene-complemented SFC neurons, Related to Figure 3. (A) Map of the pRRL-SIN-PPT-CMV-HGSNAT-ires-GFP-WPRE vector used for gene complementation, bearing the *HGSNAT* WT cDNA and the *GFP* cDNA. (B-C) *GFP* expression observed by epifluorescence in representative SNMs derived from SFC7-iPS#3.1 iPSC three days after transduction (B, scale bar: 400 µm) and in SFC7-iPS#3.1 iPSC-derived neurons differentiated for 9 weeks (C, scale bar: 50 µm). A fraction of the transduced SNMs shown in (B) were trypsinized and analyzed by flow cytometry, showing 61.6% of GFP-positive cells, compared with 0.8% of GFP-positive cells in uninfected SNMs. (D) Analyses of the HGSNAT enzyme activity expressed in log nmol/h·mg protein in neurons derived from WT (WT1-iPSC#3.6), SFC6 (SFC6-iPSC#3.1), and SFC7 (SFC7-iPSC#3.1) iPSC, differentiated 9 weeks after transduction with the vector encoding only *GFP* or the vector bearing the *HGSNAT*-ires-*GFP*. The data shows means (±S.D.) of three independent experiments performed in duplicate. ** p<0.01 (*HGSNAT*-transduced vs. corresponding culture transduced with empty vector). (E) Enlarged graph of the analyses of the HGSNAT enzyme activity of WT-, SFC6- and SFC7-cultures transduced with the vector encoding only *GFP* (corresponding to the first three bars in panel D). * p<0.05 (WT vs. patients).

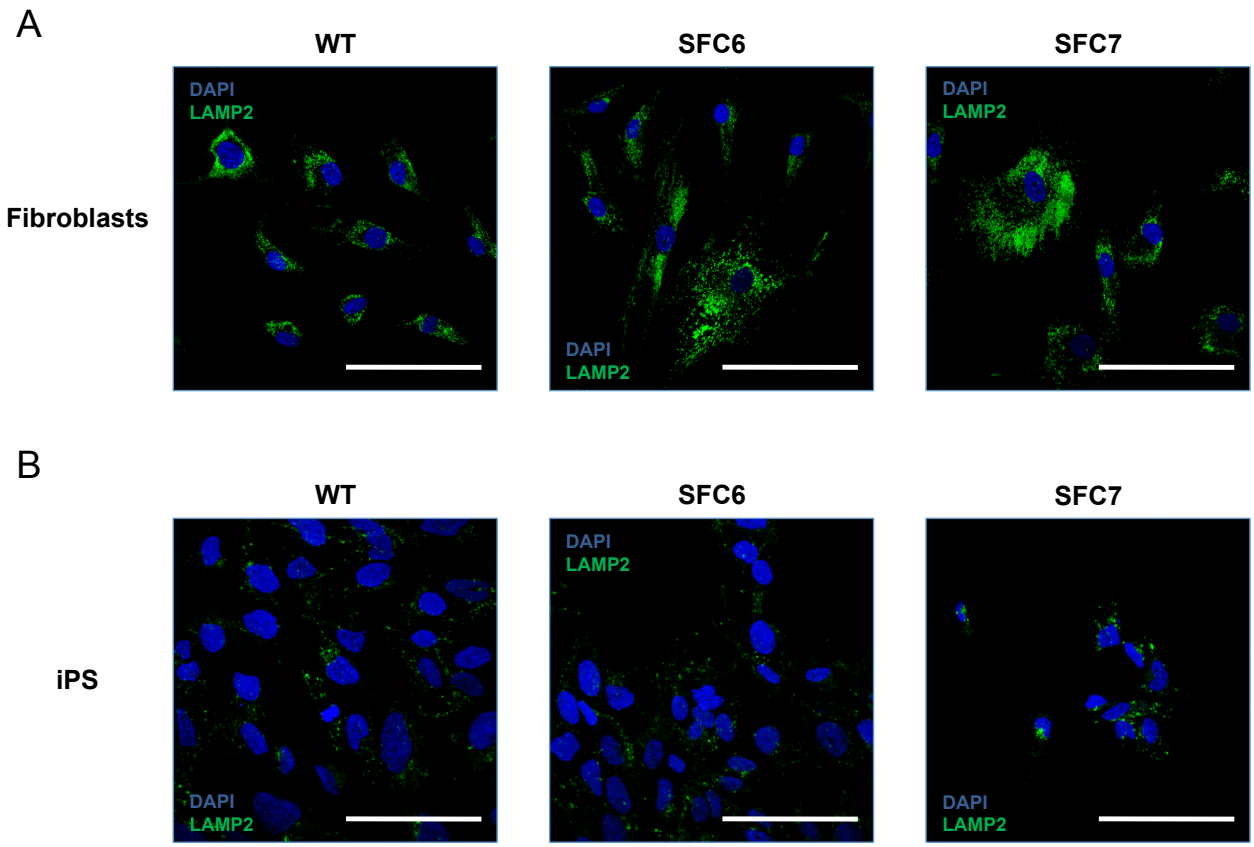

Figure S4. **Lysosome content in fibroblasts and iPSC derived from control and SFC patients, Related to Figure 4.** (A) Immunofluorescence analysis with a LAMP2 antibody in primary dermal fibroblasts from WT1 (WT), SFC6 and SFC7 individuals. Scale bar: 100 µm. (B) Immunofluorescence analysis with a LAMP2 antibody in undifferentiated iPSC generated form the same fibroblasts (lines WT1-iPSC#3.6, SFC6-iPSC#3.1, and SFC7-iPSC#3.1), showing much lower number of lysosomes, relative to that of fibroblasts. Scale bar: 100 µm.

Movie S1. Calcium imaging recording of a representative control iPSC-derived neuronal culture (line WT1-iPSC#3.6), transduced only with GFP and differentiated for 9 weeks. The field of view covers an area of 1.4 x 1 mm^2 (width x height). The real duration of the recording is 30 min. Video is accelerated 150x to show the rich spontaneous activity of the network along the measurement.

Movie S2. Calcium imaging recording of one representative SFC iPSC-derived neuronal culture (line SFC7-iPSC#3.1), transduced only with GFP and differentiated for 9 weeks. The network shows no activity. Video settings are as in Movie S1.

Movie S3. Calcium imaging recording of one representative SFC iPSC-derived neuronal culture (line SFC7-iPSC#3.1), transduced with HGSNAT-GFP lentivirus and differentiated for 9 weeks. Network activity is similar to WT conditions. Video settings are as in Movie S1.

Table S1. iPSC lines used in this study, Related to Figure 1.

Sample	Number of clones	Clone ID	Reprogr. method	AP	Karyotype	Transgene silencing	Pluripotency markers	*In vitro* differentiation	Teratoma assay	Enzyme activity
WT1	11	#3.1	3F	Passed	46, XY	Passed	Passed	Passed	Passed	Passed
		#3.6	3F	Passed	46, XY	Passed	Passed	Passed	Not tested	Passed
		#4.10	4F	Passed	46, XY	Passed	Passed	Passed	Not tested	Passed
		#4.12	4F	Passed	46, XY	Passed	Passed	Passed	Not tested	Passed
WT2	8	#3.1	3F	Passed	46, XX	Passed	Passed	Passed	Passed	Passed
		#3.2	3F	Passed	46, XX	Passed	Passed	Passed	Not tested	Passed
		#4.2	4F	Passed	46, XX	Passed	Passed	Passed	Passed	Passed
		#4.5	4F	Passed	46, XX	Passed	Passed	Passed	Not tested	Passed
SFC6	11	#3.1	3F	Passed	46, XX der(13;14)(q10;q10)	Passed	Passed	Passed	Passed	Passed
		#3.2	3F	Passed	46, XX der(13;14)(q10;q10)	Passed	Passed	Passed	Not tested	Passed
		#4.6	4F	Passed	46, XX der(13;14)(q10;q10)	Passed	Passed	Passed	Passed	Passed
		#4.7	4F	Passed	46, XX der(13;14)(q10;q10)	Passed	Passed	Passed	Not tested	Passed
SFC7	15	#3.1	3F	Passed	46, XX	Passed	Passed	Passed	Passed	Passed
		#3.2	3F	Passed	46, XX	Passed	Passed	Passed	Not tested	Passed
		#4.9	4F	Passed	46, XX	Passed	Passed	Passed	Passed	Passed
		#4.8	4F	Passed	46, XX	Passed	Passed	Passed	Not tested	Passed

Table S2. Primary and secondary antibodies used indicating working dilutions and catalog number of each one, Related to Supplemental Experimental Procedures.

Antibody	Supplier	Cat. No.	Dilution
Mouse IgG anti-OCT3/4	Santa Cruz Biotechnology	sc-5279	1:60
Rabbit IgG anti-SOX2	Pierce Antibodies	PA1-16968	1:100
Goat IgG anti-NANOG	R&D Systems	AF1997	1:25
Rat IgM anti-SSEA3	Hybridoma Bank	MC-631	1:3
Mouse IgG anti-SSEA4	Hybridoma Bank	MC-813-70	1:3
Mouse IgM anti-TRA-1-81	Millipore	MAB4381	1:200
Rabbit IgG anti-α-1-fetoprotein	Dako	A0008	1:400
Goat IgG anti-FOXA2	R&D Systems	AF2400	1:50
Rabbit IgG anti-GATA4	Santa Cruz Biotechnology	sc-9053	1:50
Mouse IgG anti-α-SMA	Sigma	A5228	1:400
Mouse IgG anti-CS	Sigma	C8035	1:400
Goat IgG anti-SOX9	R&D Systems	AF3075	1:20
Mouse IgG anti-TUJ1	Covance	MMS-435P	1:500
Rabbit IgG anti-GFAP	Dako	Z0334	1:500
Mouse IgG anti-MAP2	Sigma	M1406	1:100
Rabbit IgG anti-synapsin	Synaptic systems	106103	1:100
Mouse IgG anti-Ki67	Dako	M7240	1:100
Rabbit IgG anti-Nestin	Chemicon	AB5922	1:250
Rabbit IgG anti-PAX6	Covance	PRB-278P	1:100
Mouse IgG anti-SOX2	R&D Systems	MB2018	1:50
Mouse IgG anti-LAMP1	BD Biosciences	555801	1:10
Mouse IgG anti-LAMP2	Hybridoma Bank	H4B4	1:100
Donkey anti-rabbit IgG Cy2	Jackson ImmunoResearch	711-225-152	1:200
Donkey anti-goat IgG Cy3	Jackson ImmunoResearch	705-165-147	1:200
Donkey anti-mouse IgG AF488	Jackson ImmunoResearch	715-545-150	1:200
Donkey anti-rabbit IgG Cy3	Jackson ImmunoResearch	711-165-152	1:200
Donkey anti-mouse IgG Cy3	Jackson ImmunoResearch	715-165-151	1:200
Goat anti-rat IgM Cy3	Jackson ImmunoResearch	112-165-020	1:200
Donkey anti-goat IgG DL488	Jackson ImmunoResearch	705-485-147	1:200
Donkey anti-mouse IgM Cy3	Jackson ImmunoResearch	715-165-140	1:200
Donkey anti-mouse IgG A488	Jackson ImmunoResearch	715-545-150	1:200
Donkey anti-rabbit IgG A488	Jackson ImmunoResearch	711-225-152	1:200
Donkey anti-mouse IgM Cy2	Jackson ImmunoResearch	715-225-140	1:200
Goat anti-mouse IgG 12 ηm	Abcam	ab105286	1:30

Table S3. Primers used in this work indicating the analysis used for and their sequence, Related to Supplemental Experimental Procedures.

qPCR Total OCT4 Forward	5'-GGAGGAAGCTGACAACAATGAAA-3'
qPCR Total OCT4 Reverse	5'-GGCCTGCACGAGGGTTT-3'
qPCR Total SOX2 Forward	5'-TGCGAGCGCTGCACAT-3'
qPCR Total SO2 Reverse	5'-TCATGAGCGTCTTGGTTTTCC-3'
qPCR Total KLF4 Forward	5'-CGAACCCACACAGGTGAGAA-3'
qPCR Total KLF4 Reverse	5'-GAGCGGGCGAATTTCCAT-3'
qPCR Total c-MYC Forward	5'-AGGGTCAAGTTGGACAGTGTCA-3'
qPCR Total c-MYC Reverse	5'-TGGTGCATTTTCGGTTGTTG-3'
qPCR Trans OCT4 Forward	5'-TGGACTACAAGGACGACGATGA-3'
qPCR Trans OCT4 Reverse	5'-CAGGTGTCCCGCCATGA-3'
qPCR Trans SOX2 Forward	5'-GCTCGAGGTTAACGAATTCATGT-3'
qPCR Trans SOX2 Reverse	5'-GCCCGGCGGCTTCA-3'
qPCR Trans KLF4 Forward	5'-TGGACTACAAGGACGACGATGA-3'
qPCR Trans KLF4 Reverse	5'-CGTCGCTGACAGCCATGA-3'
qPCR Trans c-MYC Forward	5'-TGGACTACAAGGACGACGATGA-3'
qPCR Trans c-MYC Reverse	5'-GTTCCTGTTGGTGAAGCTAACGT-3'
qPCR NANOG Forward	5'-ACAACTGGCCGAAGAATAGCA-3'
qPCR NANOG Reverse	5'-GGTTCCCAGTCGGGTTCAC-3'
qPCR CRIPTO Forward	5'-CGGAACTGTGAGCACGATGT-3'
qPCR CRIPTO Reverse	5'-GGGCAGCCAGGTGTCATG-3'
qPCR REX1 Forward	5'-CCTGCAGGCGGAAATAGAAC-3'
qPCR REX1 Reverse	5'-GCACACATAGCCATCACATAAGG-3'
qPCR GAPDH Forward	5'-GCACCGTCAAGGCTGAGAAC-3'
qPCR GAPDH Reverse	5'-AGGGATCTCGCTCCTGGAA-3'
Bisulfite seq OCT4 Forward	5'-GGATGTTATTAAGATGAAGATAGTTGG-3'
Bisulfite seq OCT4 Reverse	5'-CCTAAACTCCCCTTCAAAATCTATT-3'
Bisulfite seq NANOG Forward	5'-AGAGATAGGAGGGTAAGTTTTTTTT-3'
Bisulfite seq NANOG Reverse	5'-ACTCCCACACAAACTAACTTTTATTC-3'
Integration KLF4 Forward	5'-AATTACCCATCCTTCCTGCC-3'
Integration KLF4 Reverse	5'-TTAAAAATGCCTCTTCATGTGTA-3'
Integration OCT4 Forward	5'-TAAGCTTCCAAGGCCCTCC-3'
Integration OCT4 Reverse	5'-CTCCTCCGGGTTTTGCTCC-3'
Integration SOX2 Forward	5'-AGTACAACTCCATGACCAGC-3'
Integration SOX2 Reverse	5'-TCACATGTGTGAGAGGGGC-3'
Integration c-MYC Forward	5'-TCCACTCGGAAGGACTATCC-3'
Integration c-MYC Reverse	5'-TTACGCACAAGAGTTCCGTAG-3'

Supplemental Experimental Procedures

Patients

Studies were approved by the authors' Institutional Review Board and conducted under the Declaration of Helsinki. Patients were encoded to protect their confidentiality, and written informed consent obtained. The generation of human iPS cells was done following a protocol approved by the Spanish competent authorities (Commission on Guarantees concerning the Donation and Use of Human Tissues and Cells of the Carlos III Health Institute). The two patients, SFC6 and SFC7, have been previously described (Canals et al., 2011).

Generation of iPS cells

Fibroblasts from two healthy individuals and fibroblasts from two patients were infected with retroviruses carrying human cDNA coding for *KLF4*, *SOX2*, and *OCT4* or these three cDNAs and c-*MYC* as previously described (Raya et al., 2009). Fibroblasts were mantained in DMEM (Sigma) supplemented with 10% FBS (Life Technologies) and 1% PenStrep (Life Technologies) before the infection. After the infection, fibroblasts were plated on irradiated human foreskin fibroblasts (ATCC) and maintained with hESC medium for 4-12 weeks until iPSc colonies appeared. Several clones from each cell line were obtained and validated.

Characterization of iPS cell lines

AP staining was performed using the Alkaline Phosphatase Blue Membrane Substrate Solution (Sigma). For immunocytochemistry cells were grown on HFF feeders layer for 6-10 days and then fixed in 4% PFA for 10 minutes. After EB formation, differentiation to the 3 germ layers was carried out. For endoderm, EBs were plated on 6-well plates previously treated with matrigel (BD Biosciences) for 1 hour at room temperature, and maintained for 28 days with EB medium. The same procedure was used for mesoderm, but using EB medium with 0.5 mM of Ascorbic Acid. For ectoderm differentiation, EBs were maintained in suspension for 10 days with N2B27 medium supplemented with FGF2, prepared as previously described (A

Sánchez-Danés et al., 2012). Then, EBs were plated on 6-well plates previously treated with matrigel for 1 hour at room temperature, and maintained for 21 days with N2B27 medium without FGF supplementation. Differentiated cells were fixed in 4% PFA for 10 minutes. Antibodies used are shown in Table S2. For nucleus staining DAPI (Invitrogen) at 0.5 µg/ml was used. The slides were mounted with PVA:DABCO mounting medium. Images were acquired with an SP2 confocal system (Leica) and analyzed with ImageJ software.

RT-qPCR analysis was done as previously described (Sánchez-Danés et al., 2012). All results were normalized to the average expression of Glyceraldehyde 3-phosphate dehydrogenase (GAPDH). Transcript-specific primers used are shown in Table S3.

For karyotyping, iPS cells were grown on matrigel and treated with colcemid (Life Technologies) at a final concentration of 20 ng/ml. Karyotyping analysis were carried out by Prenatal Genetics S.L. (Barcelona).

For promoter methylation, testing reprogramming genes integration and sequencing to prove that patients' iPSc were carrying mutations in *HGSNAT* gene, DNA was isolated using the QIAamp DNA Mini Kit (QIAGEN) following manufacturer's instructions. Bisulfit conversion of the promoters was carried out using the Methylamp DNA modification kit (Epigentek). Five clones of each promoter for each cell line were analyzed by sequencing. For testing genes integration, primers used are shown in Table S3. For testing mutations, primers and sequencing conditions used were the same as previously described (Canals et al., 2011).

Severe combined immunodeficient (SCID) beige mice (Charles River Laboratories) were used to test the teratoma induction capacity of patient-specific iPS cells essentially as described (Raya et al., 2008). All animal experiments were conducted following experimental protocols previously approved by the Institutional Ethics Committee on Experimental Animals, in full compliance with Spanish and European laws and regulations.

HGSNAT activity and GAGs storage

Fibroblasts, iPS cells, SNMs and cocultures with neurons and astrocytes from all the lines were harvested and enzyme activity was assayed as previously described (Canals et al., 2011). For GAGs quantification, cells were harvested using a cell scrapper and extraction of GAGs content from cells was carried out as previously described (Tolar et al., 2011) GAGs quantification were performed using the Blyscan Assay Kit (Biocolor Ltd.) following the manufacturer's instructions.

iPS differentiation to neural cells

SNMs were obtained as previously described (Cho et al., 2008). SNMs were fixed in 4% PFA for 2 hours and characterized by immunostaining. Antibodies used are shown in Table S2. For nucleus staining DAPI (Invitrogen) at 5 µg/ml was used. Mounting medium and imaging analysis were done as for *in vitro* differentiation test.

SNMs obtained from iPS-WT, iPS-SFC6 and iPS-SFC7, maintained in suspension, were then plated on slide-flasks, 6-well plates, 35mm plates or 10mm plates previously treated with matrigel for 1 hour at room temperature, and differentiated for 3, 6 or 9 weeks with N2B27 medium (Sánchez-Danés et al., 2012), without FGF supplementation to obtain the neural cultures. The correct differentiation was assessed by immunostaining. Antibodies used are shown in Table S2. For nucleus staining DAPI (Invitrogen) at 0.5 µg/ml was used. The slides were mounted with PVA:DABCO mounting medium.

Lentiviral production and transduction

The complete WT cDNA of the *HGSNAT* gene into a vector carrying an IRES-GFP construction was obtained from Simone Merlin and Antonia Follenzi (Laboratory of Histology, Department of Medical Service, University of Piemonte Orientale "A. Avogadro", Novara, Italy) and named pRRL-SIN-PPT-CMV-HGSNAT-ires-GFP-WPRE. High-titer VSV-pseudotyped LV stocks were produced in 293T cells by calcium phosphate-mediated transient transfection of the transfer vector pRRL-SIN-PPT-CMV-HGSNAT-ires-GFP-WPRE, the late generation packaging construct pMDL

and the VSV envelope-expressing construct pMD2.G, and purified by ultra-centrifugation as previously described (Consiglio et al., 2004). Tritation of the virus was carried out using 293T cells and analyzed by FACS, obtaining 2.9 x 10^9 TU/mL for the control virus and 5.4 x 10^8 TU/mL for the virus carrying the correction. Transduction was carried out in the SNM step, using 1 µl of *GFP* virus and 3µl of *HGSNAT-GFP* virus.

Transmission electron microscopy

Neurons and astrocytes cocultures were grown on 10mm plates as described above for 3, 6 and 9 weeks. Fibroblasts and iPSc were grown until subconfluence. Cells were fixed with 2.5% glutaraldehyde for 90 minutes and then collected and treated with 0.1M osmium for 2 hours. Dehydratation was carried out with acetone and blocks were obtained with Epon. For cryoultramicrotomy and posterior immunogold staining, neurons and astrocytes, fibroblasts and iPSc were fixed with 4% PFA and 0.1% glutaraldehyde, washed with 0.15M glycine, treated with 12% gelatin, cryoprotected with 2.3M sucrose and cyrofixed with liquid nitrogen. Antibodies used are shown in Table S2. Images were acquired with a transmission microscopy JEOL1010 and analyzed with ImageJ software.

Calcium fluorescence imaging

We used calcium imaging (Orlandi et al., 2013; Takahashi et al., 2010; Takahashi et al., 2007; Tibau et al., 2013) to evaluate the differences in spontaneous activity between healthy and Sanfilippo's affected neuronal cultures. This technique uses a fluorescence probe to reveal the fast increase of calcium levels inside neurons upon firing. Several studies have shown that the emitted fluorescence captures well the action potentials elicited by the cells (Chen et al., 2013; Sasaki et al., 2008; Smetters et al., 1999). Although measurements of neuronal activity are more precise with patch clamp, electrodes or other techniques, calcium imaging allows the monitoring of a large population of neurons, simultaneously and non-invasively, which makes it particularly suitable for whole network analyses.

The studied cultures were prepared as described before. For each condition (WT, SFC6, and SFC7) we prepared 27 identical cultures. Nine of them were later transduced with *HGSNAT-GFP*, nine were transduced with *GFP* only and the rest remained untransduced. We then investigated the behavior of the cultures at 3, 6, and 9 weeks after plating. For each preset time, we measured the spontaneous activity in 3 *HGSNAT-GFP*-transfected, in 3 *GFP*-transfected and in 3 untransfected cultures, for 30 minutes.

Prior to imaging, the culture dish to study was first gently washed with 4ml PBS at room temperature to remove the original culture medium. Next, we incubated the cultures for 30 min in a solution that contained 1ml of recording medium (RM, consisting of 128 mM NaCl, 1 mM $CaCl_2$, 1 mM $MgCl_2$, 45 mM sucrose, 10 mM glucose, and 0.01 M Hepes; treated to pH 7.4) and 4 μg/ml of the cell-permeant calcium sensitive dye Fluo-4-AM. At the end of incubation we washed the culture with 2 ml of fresh RM to remove residual free Fluo-4. This medium was discarded to place 4 ml of fresh RM, the final medium for actual recordings.

The culture dish was mounted on a Zeiss inverted microscope equipped with a CMOS camera (Hamamatsu Orca Flash 2.8) and an arc lamp for fluorescence. Grey-scale images of neuronal activity were acquired at intervals of 50 ms, with a size of 960x720 pixels and a spatial resolution of 2.90 μm/pixel. The latter settings provided a final field of view of 2.8x2.1 mm that contained between 150 and 300 neurons.

For each recorded culture we extracted the fluorescence amplitude of all neurons in the field of view as a function of time. Neuronal firing events were detected as a fast rise in the fluorescence signal, as illustrated in the traces of Figure 5A.

Fluorescence time series were finally analyzed to determine two network activity descriptors, namely the ‘fraction of active neurons’ and the ‘network activity’. We first defined active cells as those that showed, during the 30 min duration of the recording, at least a firing event of amplitude larger than two times the amplitude of the noise. The events with the lowest amplitude corresponded to single spikes, while larger amplitudes corresponded to fast spike trains or ‘bursts’. Since single spikes were in general difficult to discern given the inherent fluctuations in the signal, we considered solely as active those neurons that exhibited neat bursting episodes.

These bursts are prominent in healthy, WT cultures, and therefore, their quantification provides a good estimate of the degradation of the cultures upon disease. The ‘fraction of active neurons’ in the network was therefore computed as the ratio between the number of cells showing at least a burst and the total population monitored. The average ‘network activity’ was determined as the number of observed bursting events divided by the total number of monitored cells. The latter quantity is our main measure of the health of the neuronal network.

Data was finally averaged among the 3 replicates of each time-point and transduction. Hence, our results are based on a statistics of at least 450 neurons per time-point and transduction.

Supplemental References

Chen, T.-W., Wardill, T.J., Sun, Y., Pulver, S.R., Renninger, S.L., Baohan, A., Schreiter, E.R., Kerr, R.A, Orger, M.B., Jayaraman, V., et al. (2013). Ultrasensitive fluorescent proteins for imaging neuronal activity. Nature 499, 295–300.

Consiglio, A., Gritti, A., Dolcetta, D., Follenzi, A., Bordignon, C., Gage, F.H., Vescovi, A.L., and Naldini, L. (2004). Robust in vivo gene transfer into adult mammalian neural stem cells by lentiviral vectors. *Proc. Natl. Acad. Sci. U. S. A*. *101*, 14835–14840.

Orlandi, J.G., Soriano, J., Alvarez-Lacalle, E., Teller, S., and Casademunt, J. (2013). Noise focusing and the emergence of coherent activity in neuronal cultures. Nat. Phys. 9, 582–590.

Raya, A., Rodríguez-Pizà, I., Arán, B., Consiglio, A., Barri, P.N., Veiga, A., and Izpisúa Belmonte, J.C. (2008). Generation of cardiomyocytes from new human embryonic stem cell lines derived from poor-quality blastocysts. *Cold Spring Harb. Symp. on Quant. Biol*. *73*, 127–135.

Sánchez-Danés, A., Consiglio, A., Richaud, Y., Rodríguez-Pizà, I., Dehay, B., Edel, M., Bové, J., Memo, M., Vila, M., Raya, A., and Izpisua Belmonte, J.C. (2012). Efficient generation of A9 midbrain dopaminergic neurons by lentiviral delivery of LMX1A in human embryonic stem cells and induced pluripotent stem cells. *Hum. Gene Ther*. *23*, 56–69.

Sasaki, T., Takahashi, N., Matsuki, N., and Ikegaya, Y. (2008). Fast and accurate detection of action potentials from somatic calcium fluctuations. J. Neurophysiol. 100, 1668–1676.

Smetters, D., Majewska, A., and Yuste, R. (1999). Detecting action potentials in neuronal populations with calcium imaging. Methods 18, 215–221.

Takahashi, N., Sasaki, T., Usami, A., Matsuki, N., and Ikegaya, Y. (2007). Watching neuronal circuit dynamics through functional multineuron calcium imaging (fMCI). Neurosci. Res. 58, 219–225.

Takahashi, N., Takahara, Y., Ishikawa, D., Matsuki, N., and Ikegaya, Y. (2010). Functional multineuron calcium imaging for systems pharmacology. Anal. Bioanal. Chem. 398, 211–218.

Tibau, E., Valencia, M., and Soriano, J. (2013). Identification of neuronal network properties from the spectral analysis of calcium imaging signals in neuronal cultures. Front. Neural Circuits 7, 199.